

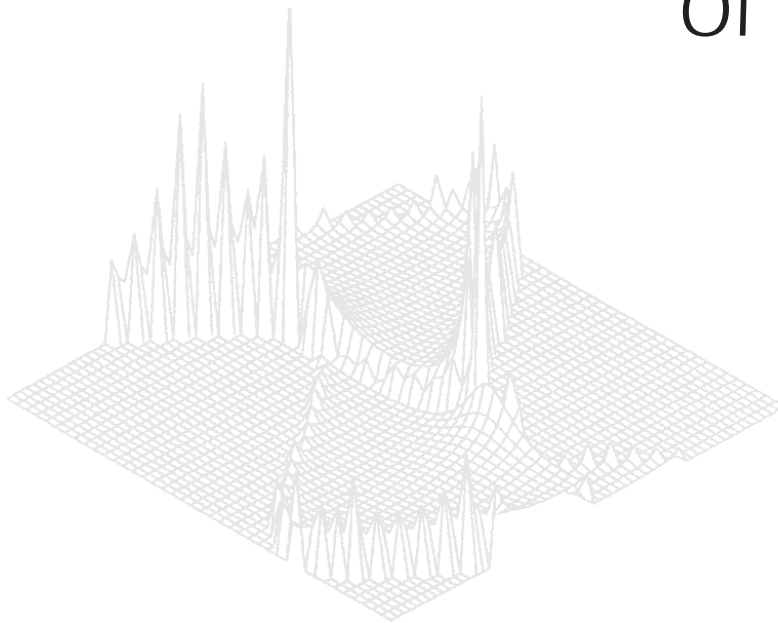
---

**C S I R O   P U B L I S H I N G**

---

# Australian Journal of Physics

Volume 51, 1998  
© CSIRO 1998



A journal for the publication of  
original research in all branches of physics

**[www.publish.csiro.au/journals/ajp](http://www.publish.csiro.au/journals/ajp)**

All enquiries and manuscripts should be directed to

*Australian Journal of Physics*

**CSIRO PUBLISHING**

PO Box 1139 (150 Oxford St)

Collingwood

Vic. 3066

Australia

Telephone: 61 3 9662 7626

Facsimile: 61 3 9662 7611

Email: [peter.robertson@publish.csiro.au](mailto:peter.robertson@publish.csiro.au)



Published by **CSIRO PUBLISHING**  
for CSIRO and the  
Australian Academy of Science



## Neutron Diffraction Study of Tetragonal Zirconias containing Tetravalent Dopants

B. A. Hunter,<sup>A</sup> C. J. Howard<sup>A</sup> and D.-J. Kim<sup>B</sup>

<sup>A</sup> Australian Nuclear Science and Technology Organisation, Private Mail Bag 1, Menai, NSW 2234, Australia.

<sup>B</sup> Ceramics Division, Korea Institute of Science and Technology, Seoul 136–791, Korea.

### *Abstract*

In tetragonal zirconia, the cation is coordinated by two interpenetrating tetrahedra of oxygen ions, implying two different cation–oxygen bond lengths. Neutron powder diffraction was used to study tetragonal  $ZrO_2$ –2 mol%  $Y_2O_3$  incorporating various amounts of the different tetravalent ions Ge, Ti, Sn and Ce. Precise and accurate values for the lattice parameters and the variable oxygen position parameter have been obtained, and from these the bond lengths derived. The results are compared with those from an earlier X-ray and Raman study on the same materials. Of interest are the confirmation of the increase in cell volume occurring when Zr is replaced by the smaller Sn ion, and the observation of departures from Vegard's law in the case of substitution of Zr by Ti.

### 1. Introduction

Zirconia and zirconia alloys find widespread application as engineering ceramics, and have for this reason been extensively studied (Hannink and Swain 1994; Green *et al.* 1988). In this context the tetragonal form of zirconia attracts much attention because it is the martensitic transformation from metastable tetragonal to monoclinic zirconia under applied stresses that gives rise to transformation toughening (Green *et al.* 1988). Tetragonal zirconia alloys in ternary oxide systems have been the subject of several studies aimed at understanding the factors influencing the stability of the tetragonal phase (Kim *et al.* 1993; Kim and Tien 1991; Kim 1990; Lin *et al.* 1990; Pydra *et al.* 1991; Wilson and Glasser 1989; Li *et al.* 1994).

In this paper we report on a neutron powder diffraction study of tetragonal  $ZrO_2$ –2 mol%  $Y_2O_3$  doped with various amounts of  $CeO_2$ ,  $SnO_2$ ,  $TiO_2$  or  $GeO_2$ . Similar samples had been studied previously by Kim *et al.* (1997), who measured lattice parameters using a laboratory X-ray diffractometer, and carried out comprehensive Raman investigations. The solubility limits for the different oxides in the tetragonal phase were determined from an inspection of the X-ray and Raman data. The change in the frequency of a particular Raman mode gave an indication of the change in length with composition of the shorter cation–oxygen bond, but there was no such indication for the longer bond because the frequency of the relevant Raman mode was dominated by other factors. In the case of Sn substituted materials the X-ray and Raman study gave an intriguing result: though the Sn has a smaller ionic radius than the Zr ion, and the Raman shift

**Table 1. Structural parameters of (ZrO<sub>2</sub>/2 mol% Y<sub>2</sub>O<sub>3</sub>)-MO<sub>2</sub> mol% from neutron diffraction data for M = Ce, Sn, Ti and Ge**

Here  $\delta$  is the deviation of the oxygen position parameter from the value it would have in the ideal fluorite structure and  $\chi^2$  is the goodness of fit. The numbers in parentheses are the estimated standard deviations of the last significant figures

Sample	$a$ (Å) <sup>A</sup>	$c$ (Å)	$\delta$	$n(\text{O})$	$B_{\text{Zr}}$ (Å <sup>2</sup> )	$B_{\text{O}}$ (Å <sup>2</sup> )	$V^{\frac{1}{3}}$ (Å)	$d_{\text{s}}^{\text{Zr-O}}$ (Å) <sup>B</sup>	$d_{\text{1}}^{\text{Zr-O}}$ (Å) <sup>B</sup>	Second phase <sup>C</sup>	$\chi^2$
0%	5.0969(1)	5.1804(2)	0.0433(1)	0.992(8)	0.25(2)	0.57(2)	5.1246(2)	2.096(1)	2.357(1)	—	3.25
Ce 4%	5.1093(1)	5.1902(2)	0.0426(1)	1.004(8)	0.31(3)	0.81(3)	5.1361(2)	2.103(1)	2.360(1)	—	3.05
Ce 8	5.1241(1)	5.2023(2)	0.0416(1)	1.000(8)	0.33(3)	0.80(2)	5.1501(2)	2.111(1)	2.363(1)	—	2.97
Ce 12%	5.1359(1)	5.2117(2)	0.0408(1)	1.000(8)	0.47(3)	1.08(3)	5.1611(3)	2.118(1)	2.365(1)	—	3.04
Ce 16%	5.1479(1)	5.2227(2)	0.0392(1)	0.996(8)	0.40(3)	0.88(3)	5.1727(3)	2.127(1)	2.365(1)	6% c-ZrO <sub>2</sub>	2.96
Sn 2%	5.0966(1)	5.1857(2)	0.0444(1)	1.000(8)	0.49(3)	0.98(3)	5.1261(3)	2.094(1)	2.362(1)	—	2.46
Sn 4%	5.1912(2)	5.1912(2)	0.0452(1)	1.008(8)	0.50(3)	1.06(3)	5.1276(3)	2.092(1)	2.365(1)	—	2.45
Sn 6%	5.0958(1)	5.1968(2)	0.0461(1)	1.012(8)	0.58(3)	1.19(3)	5.1293(3)	2.090(1)	2.369(1)	—	2.62
Sn 8%	5.0956(1)	5.2029(2)	0.0471(1)	1.012(8)	0.61(3)	1.21(3)	5.1311(3)	2.088(1)	2.374(1)	—	2.58
Sn 10%	5.0953(1)	5.2040(2)	0.0480(1)	1.004(8)	0.59(3)	1.21(3)	5.1313(3)	2.086(1)	2.377(1)	2% SnO <sub>2</sub>	2.62
Ti 4%	5.0696(1)	5.1836(2)	0.0458(1)	1.004(8)	0.53(3)	1.11(3)	5.1209(2)	2.088(1)	2.364(1)	—	2.50
Ti 8%	5.0810(1)	5.1879(2)	0.0480(1)	1.004(8)	0.59(3)	1.44(3)	5.1164(2)	2.080(1)	2.370(1)	—	2.53
Ti 12%	5.0714(1)	5.1939(2)	0.0508(1)	0.996(8)	0.63(3)	1.63(3)	5.1119(3)	2.070(1)	2.378(1)	—	2.56
Ti 16%	5.0612(1)	5.2014(2)	0.0534(1)	0.996(10)	0.85(3)	2.11(3)	5.1075(4)	2.061(1)	2.386(1)	—	2.88
Ti 20%	5.0557(1)	5.2045(2)	0.0557(1)	0.952(10)	0.97(3)	2.36(3)	5.1048(4)	2.054(1)	2.405(1)	3% ZrTiO <sub>4</sub>	3.38
Ge 1%	5.0944(1)	5.1806(2)	0.0442(1)	0.988(10)	0.38(3)	0.76(3)	5.1230(3)	2.093(1)	2.360(1)	—	3.24
Ge 2%	5.0930(1)	5.1808(2)	0.0443(1)	1.008(8)	0.37(3)	0.91(3)	5.1221(3)	2.092(1)	2.359(1)	—	3.21
Ge 3%	5.0909(1)	5.1804(2)	0.0447(1)	1.000(8)	0.41(3)	1.00(3)	5.1206(3)	2.090(1)	2.360(1)	—	3.02

<sup>A</sup> Dimension of the face-centred fluorite like cell.

<sup>B</sup> Calculated using  $d_{\text{s}}^{\text{Zr-O}} = [\frac{1}{8}a^2 + c^2(\frac{1}{4} - \delta)^2]^{\frac{1}{2}}$  and  $d_{\text{1}}^{\text{Zr-O}} = [\frac{1}{8}a^2 + c^2(\frac{1}{4} + \delta)^2]^{\frac{1}{2}}$  (Howard *et al.* 1998).

<sup>C</sup> Molar percentage.

indicated that the mean length of the shorter cation–anion bond decreases as the concentration of Sn is increased, the unit cell volume increased with increasing concentration of Sn. The purposes of our neutron study were to determine both lattice parameters and oxygen position parameter, and from these to derive accurate values for the bond lengths.

## 2. Experimental and Data Analysis

Samples with the compositions indicated in Table 1 were prepared by adding pure (99.9%) CeO<sub>2</sub>, GeO<sub>2</sub>, TiO<sub>2</sub> or SnO<sub>2</sub> into commercially available ZrO<sub>2</sub>–2 mol% Y<sub>2</sub>O<sub>3</sub> powder (Tosoh Inc., Japan). After mixing, drying, calcining and subsequent milling, pellets for neutron diffraction of approximately 4 g each were prepared by pressing and sintering at 1500°C for 1 hour, except for the samples with Ge that were sintered for 3 hours at 1350°C (Kim *et al.* 1997).

Neutron powder diffraction data were collected using the High Resolution Powder Diffractometer (HRPD) at the HIFAR reactor at the Australian Nuclear Science and Technology Organisation (Howard *et al.* 1983). The HRPD now carries 24 detectors. Patterns were recorded using 1.493 Å neutrons over a range  $0 < 2\theta < 154^\circ$  in  $0.05^\circ$  steps. Rietveld analysis of the data was carried out using a modified version of the LHPM program (Hill and Howard 1986).

The refinements of the tetragonal phases were carried out in space group  $P4_2/nmc$  (No. 137). The structure consists of a cation (Zr/Y/M) on the  $2a(\frac{3}{4}, \frac{1}{4}, \frac{3}{4})$  atomic site and an anion (O) at the  $4d(\frac{1}{4}, \frac{1}{4}, z)$  position. The parameters

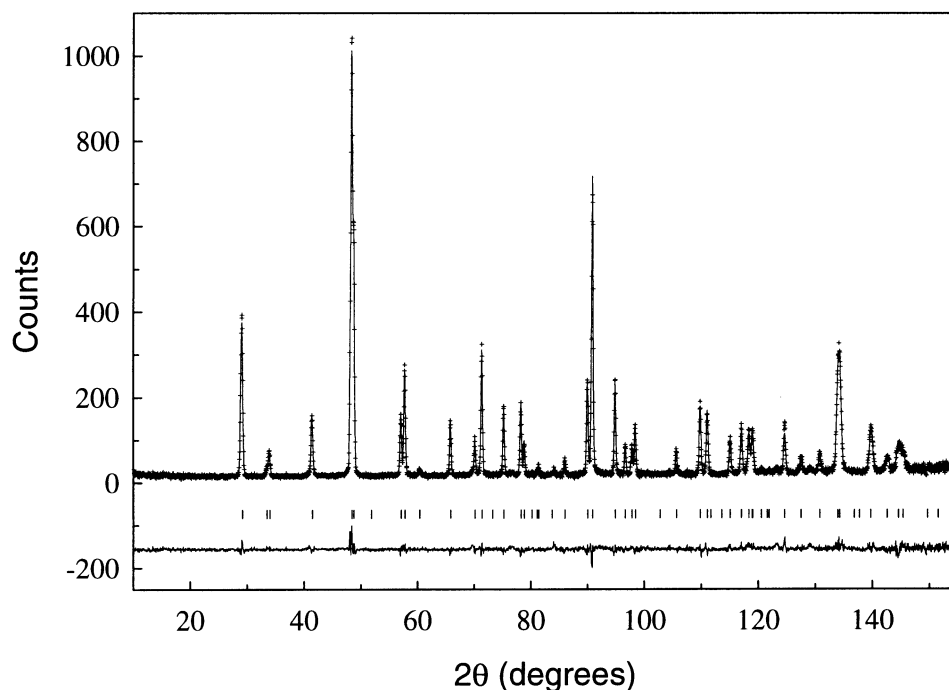


**Fig. 1.** Plot of the neutron diffraction data and Rietveld fit from the 8 mol% Ce doped tetragonal zirconia sample. The crosses are the measured data, the line through the data is the Rietveld fit, and the line below is the difference. The markers represent the Bragg reflections from the tetragonal zirconia phase.

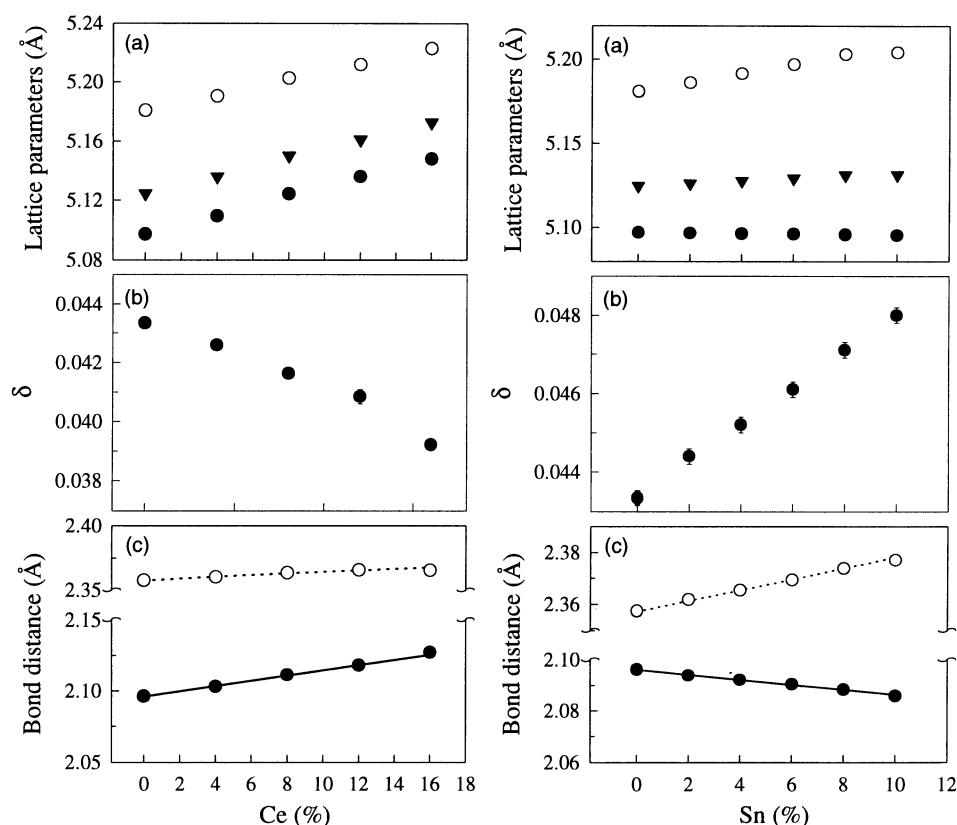


**Fig. 2.** Dependence of (a) lattice parameters  $a$  (solid circles),  $c$  (open circles) and the cube root of the unit cell volume (triangles); (b) the oxygen parameter  $\delta$ ; and (c) the short and long bond lengths on composition for various tetravalent dopants. The continuous line in (c) is the linear regression fit, and the broken line is from a bond valence sum analysis (Hunter *et al.* 1998).

refined included the lattice parameters ( $a$  and  $c$ ), the oxygen positional parameter, the oxygen occupancy, and the isotropic thermal parameters for the Zr and O sites. Anisotropic thermal parameters were refined but gave no significantly better fits, and consequently, the thermal parameters were refined isotropically for the final fits. The oxygen position is conveniently indicated by its deviation,  $\delta = 0.5 - z$ , from the position it would have in the cubic fluorite. The peak shape was described by a Voigt function, where the width of the Gaussian component varied as  $\text{FWHM}_{\text{Gauss}} = [U \tan^2 \theta + V \tan \theta + W]^{\frac{1}{2}}$ , and the Lorentzian component varied according to a particle size model,  $\text{FWHM}_{\text{Lorentz}} = \kappa \sec \theta$ . The background was described by a third order polynomial and was refined simultaneously with the other parameters. The plot obtained from Rietveld refinement of the 8 mol% Ce sample is shown in Fig. 1.

Certain samples with higher concentrations of substituents contained secondary phases. After identification, these phases were incorporated into the Rietveld refinement, and the amounts determined (Hill and Howard 1987).

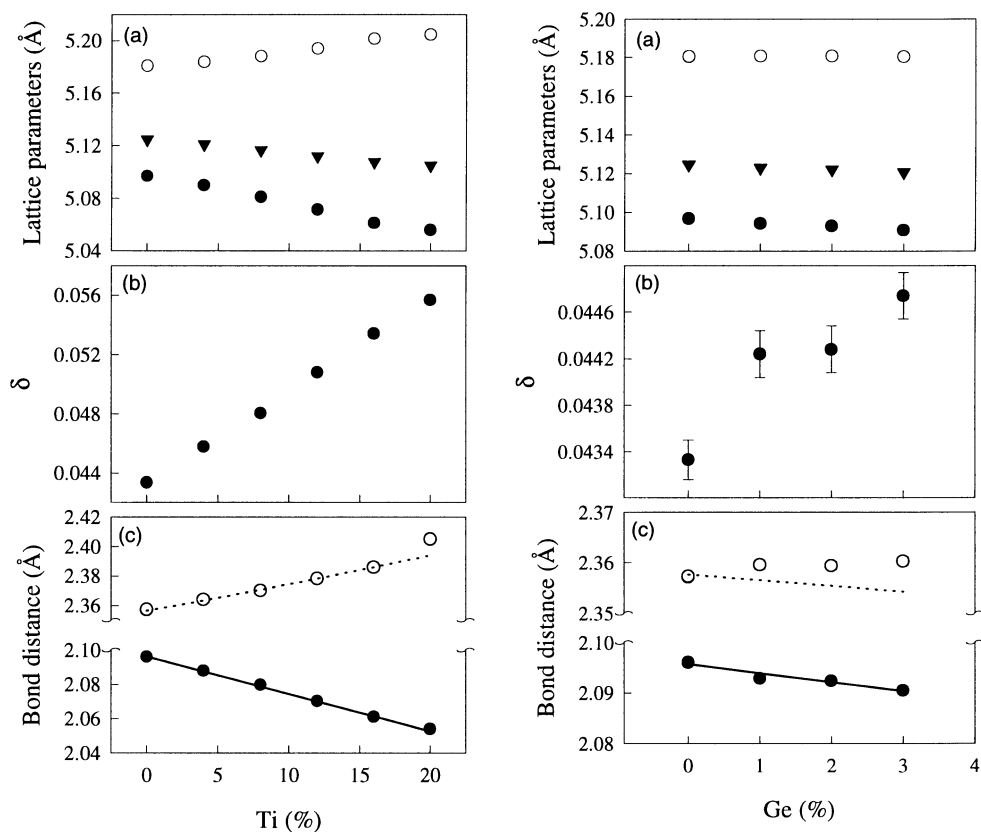


Fig. 2. (Continued)

### 3. Results and Discussion

The principal results from the analysis are the lattice parameters,  $a$  and  $c$ , and the parameter  $\delta$  describing the oxygen position. These results are presented in Table 1 along with the oxygen occupancy and the isotropic thermal parameters. The variations of  $a$ ,  $c$  and  $\delta$  with composition for the various substituents are shown in Fig. 2. The derived values of the cube root of the unit cell volume ( $a^2c$ )<sup>1/3</sup> and the two cation-anion bond lengths are also tabulated in Table 1 and plotted in Fig. 2.

The refined values of the occupation of the oxygen site (Table 1), in every case, were consistent with a vacancy concentration to be expected from the presence of 2 mol% Y<sub>2</sub>O<sub>3</sub> in the samples. This result is of interest in view of a suggestion by Kountourous and Petzow (1993) that there may be vacancies associated with Ce substitution. These authors argued that the stability of the tetragonal (and then the cubic) phase depends on the presence of oxygen vacancies, which they would attribute to the partial reduction of Ce<sup>4+</sup> to Ce<sup>3+</sup> during sintering. The current study is conclusive in that no systematic variation in the oxygen vacancy was observed in any of the samples, so the argument that oxygen vacancies are introduced with tetravalent dopants cannot be sustained.

Thermal parameters can sometimes be used as an indication of static disorder, in particular in doped systems such as examined here. The isotropic thermal parameters were refined and for the starting material,  $\text{ZrO}_2$ -2 mol%  $\text{Y}_2\text{O}_3$ , were  $B_{\text{Zr}} = 0.24 \text{ \AA}^2$  and  $B_{\text{O}} = 0.57 \text{ \AA}^2$ . With increasing concentration of substituent the thermal parameters increased reaching a high of  $B_{\text{Zr}} = 0.97 \text{ \AA}^2$  and  $B_{\text{O}} = 2.36 \text{ \AA}^2$  in the Ti system. Not unexpectedly the variation of thermal parameters reflected the difference in the ionic size of the substituent in relation to the ionic size of Zr.

It of interest to compare the results (Fig. 2) with those obtained in the X-ray and Raman study by Kim *et al.* (1997). In the present study, we noted evidence of second phases in the 16 mol% Ce, 10 mol% Sn and 20 mol% Ti samples, indicative of solubility limits. These are in agreement with those determined by the Raman study (Kim *et al.* 1997).

Lattice parameters from our neutron study are in good agreement, as they should be, with the X-ray lattice parameters. For the Ti substituted material (ignoring the point at 20 mol% affected by the second phase), the study reveals nonlinearity in the variation of both the lattice parameters with composition. The variation of the cube root of the cell volume, however, is linear.

**Table 2.** Effect of substitution on the short bond length  $d_{\text{s}}^{\text{Zr-O}}$  from linear regression analysis

The rms deviation is a measure of the fit. The numbers in parentheses are estimated standard deviations of the last significant figures

Element ion	$d_{\text{s}}^{\text{Zr-O}}$ ( $x = 0$ ) (Å)	$d(d_{\text{s}}^{\text{Zr-O}})/dx$ (Å mol% <sup>-1</sup> )	rms deviation (Å)
Zr <sup>4+</sup>	—	0.0	—
Ge <sup>4+</sup>	2.0956(7)	$-1.81(34) \times 10^{-3}$	0.00056
Ti <sup>4+</sup>	2.0965(4)	$-2.18(4) \times 10^{-3}$	0.00039
Sn <sup>4+</sup>	2.0960(1)	$-0.98(2) \times 10^{-3}$	0.00012
Ce <sup>4+</sup>	2.0959(4)	$1.84(6) \times 10^{-3}$	0.00038

The main point of the neutron investigation was to determine accurate values for the bond lengths. The results for the short bond show its length increasing upon substituting Ce, but decreasing for Sn, Ti and Ge substitution. These results are in accord with the Raman shift of the  $640 \text{ cm}^{-1}$  mode (Kim *et al.* 1997). It is apparent in Fig. 2 that the length of the shorter bond varies linearly with substituent concentration. Linear regression analysis has been carried out on the bond length data (omitting points affected by secondary phases), and the results are given in Table 2. The slopes are positive for Ce, which has a larger ionic radius than Zr, and negative for substitution of Zr by the smaller Sn, Ti and Ge ions. The slopes are nearly linearly dependent on ionic radius, the exception being Ge which is typically covalent. The fact that the short bond length decreases upon substituting Sn, yet the cell volume increases, has been established in this work.

The longer bond length, not accessible in the Raman study (Kim *et al.* 1997), has also been determined in this work. It has been found that the variation in the length of this bond can be accounted for by charge balance effects (Hunter *et al.* 1998), as expressed by the requirement that the bond valence sum remains

constant. This provides an explanation for the 'anomalous' behaviour in the case of substitution of Zr by Sn: as the shorter bond gets shorter, the longer bond is driven to become longer (at a greater rate), and an increase in cell volume results.

#### 4. Summary

The neutron measurements reported here, and the bond lengths derived from them, have led to greater insight into the factors determining the details of the structures of tetragonal zirconias. The question of what stabilises these structures, however, is still to be resolved.

#### Acknowledgments

We acknowledge useful discussions with Dr E. H. Kisi (University of Newcastle) during the course of this work. The authors would also like to acknowledge Dr M. V. Swain (CSIRO, Division of Applied Physics) for his part in promoting this collaboration.

#### References

- Green, D. J., Hannink, R. H. J., and Swain, M. V. (1988). 'Transformation Toughening of Ceramics' (CRC Press: Boca Raton, FL).
- Hannink, R. H. J., and Swain, M. V. (1994). *Annu. Rev. Mater. Sci.* **24**, 359.
- Hill, R. J., and Howard, C. J., (1986). A computer program for Rietveld analysis of fixed wavelength X-ray and neutron powder diffraction patterns. Rep. No. AAEC/M112, AAEC, Lucas Heights.
- Hill, R. J., and Howard, C. J. (1987). *J. Appl. Crystallogr.* **20**, 467.
- Howard, C. J., Ball, C. J., Davis, R. L., and Elcombe, M. M. (1983). *Aust. J. Phys.* **36**, 507.
- Howard, C. J., Hunter, B. A., and Kim, D.-J. (1998). *J. Am. Ceram. Soc.* **81**, 241.
- Hunter, B. A., Howard, C. J., and Kim, D.-J. (1998). to be published.
- Kim, D.-J. (1990). *J. Am. Ceram. Soc.* **73**, 115.
- Kim, D.-J., and Tien, T. Y. (1991). *J. Am. Ceram. Soc.* **74**, 3061.
- Kim, D.-J., Jang, J. W., and Lee, H. L. (1997). *J. Am. Ceram. Soc.* **80**, 1453.
- Kim, D.-J., Jung, H. J., and Yang, I. S. (1993). *J. Am. Ceram. Soc.* **76**, 2106.
- Kountouros, P. and Petzow, G. (1993). In 'Science and Technology of Zirconia V' (Eds S. P. S. Badwal *et al.*) (Technomic Publishing: Lancaster, PA, USA).
- Li, P., Chen, I.-W., and Penner-Hahn, J. E. (1994). *J. Am. Ceram. Soc.* **77**, 1289.
- Lin, C. L., Gan, D., and Shen, P. (1990). *Mat. Sci. Eng. A* **129**, 147.
- Pydra, W., Haberk, K., Bucko, M. M., and Faryna, M. (1993). In 'Science and Technology of Zirconia V' (Eds S. P. S. Badwal *et al.*) (Technomic Publishing: Lancaster, PA, USA).
- Wilson, G., and Glasser, F. P. (1989). *Br. Ceram. Trans. J.* **88**, 69.